Electronic Dephasing in Bimetallic Gold−Silver Nanoparticles Examined by Single Particle Spectroscopy

Xuan Wang, Zhenyuan Zhang, and Gregory V. Hartland*

Department of Chemistry and Biochemistry, University of Notre Dame, Notre Dame, Indiana 46556-5670

Received: July 30, 2005; In Final Form: September 7, 2005

The scattering spectra of single gold, silver, and bimetallic gold−silver particles (both core−shell and alloyed) have been examined using dark-field microscopy. The results show that the plasmon resonances for the bimetallic particles are broader than those of the pure silver or pure gold particles. However, plots of the width of the plasmon resonance vs resonance frequency for the core−shell and alloyed samples are very similar. This implies that the broadening is due to the frequency dependence of the dielectric constants of the particles. For the core−shell particles, scattering at the interface between the two metals does not seem to be a significant effect.

1. Introduction

Understanding the effects of size confinement on the optical properties of metal particles has a long history in chemical physics.[1] The classical observation is that the plasmon resonance of the particles becomes broader as the particle size decreases,[2−6] due to the dephasing of the electron motion induced by surface scattering.[7−10] Because the position of the plasmon resonance for metal particles is relatively insensitive to size,[1] spectral broadening due to polydispersity in the samples is not a problem. Thus, these experiments are relatively easy to perform. The spectra can be recorded with a standard UV−vis spectrometer, and there are no special requirements for making the samples: recipes developed over 100 years ago (for example) can be used to see the effect.[11] This statement is not meant to down play the significance of these early experiments: this work is very elegant and represents the start of nanoscience as studied through the properties of clusters.

The surface scattering induced broadening of the plasmon resonance in metal particles can be theoretically accounted for by adding a size-dependent damping term to the dielectric constants of the particles.[1,7−10] The way this is done is to split the dielectric constant into intraband (ϵ^{f}) and interband (ϵ^{ib}) contributions. For particles larger than a few nanometers, all the size dependence is contained in ϵ^{f}.[1] The intraband (free electron) contributions are calculated using the Drude model[12]

$$\epsilon_1^{f}(\omega) = 1 - \frac{\omega_p^2}{\omega^2 + \gamma^2}$$

$$\epsilon_2^{f}(\omega) = \frac{\omega_p^2 \gamma}{\omega(\omega^2 + \gamma^2)} \qquad (1)$$

where ϵ_1 and ϵ_2 are the real and imaginary components of the dielectric constant, ω_p is the plasma frequency, and γ is the damping constant. In these equations, the plasma frequency is given by $\omega_p = (Ne^2/m_e\epsilon_o)^{1/2}$, where N is the free electron density and m_e is the effective mass of the electrons. Surface scattering of the conduction electrons is included by writing $\gamma = \gamma_b + Av_F/L_{eff}$ where v_F is the Fermi velocity, γ_b is the damping constant for bulk metal, L_{eff} is the effective mean free path of the electrons, and A is a constant, which is on the order of unity.[1,8−10] The value of L_{eff} depends on the shape of the particles, and a general expression (recently derived by Schatz and co-workers) is $L_{eff} = 4V/S$, where V is the volume of the particle and S is the surface area.[13] For spherical particles this gives $L_{eff} = 4R/3$, where R is the radius. For gold, the contribution from surface scattering is approximately equal to the bulk damping constant for particles with $R \approx 1.5$ nm and surface damping is negligible for $R > 10$ nm.[1]

Recently, there has been considerable interest in examining the spectra of single metal particles.[14−23] The easiest way to do this is to record Rayleigh scattering spectra using an optical microscope with either dark-field or total-internal reflection illumination.[14−19] Metal particles scatter light very strongly: scattering from single silver or gold particles larger than 20 nm diameter can be easily seen by the eye under a micrscope. Most of these studies have concentrated on determining how the position of the plasmon resonance depends on the size, shape, and environment of the particles. The effect of size confinement on the width of the spectra has not been studied. The main reason for this is that the scattering efficiency is proportional to R^6, which means that small particles are very hard to study. Absorption-based spectroscopy techniques have recently been developed for studies of single (nonfluorescent) particles;[20−23] however, a systematic study of the absorption spectra of small metal particles has not been reported to date.

Several single particle studies have addressed the width of the plasmon resonance.[15,16,19] Feldmann and co-workers examined the width of the scattering spectra for large spherical particles of silver and gold (diameters > 20 nm) and nanorods of gold (aspect ratios up to 4 and widths on the order of 20 nm).[15,16] They found that for a given resonance frequency the rods have much narrower spectra than the spheres. This is due to electromagnetic retardation effects for the spherical particles,[1] which produce a significant broadening of the plasmon resonance for diameters greater than 40 nm. For the spheres, the widths of the measured spectra were in good agreement with

* To whom correspondence should be addressed. Tel: 574-631-9320. Fax: 574-631-6652. E-mail: hartland.1@nd.edu. Webpage: www.nd.edu/~ghartlan.

10.1021/jp054233u CCC: $30.25
Published on Web 10/11/2005

that calculated using the full Mie theory expression for scattering.[24] For the rods, the width of the longitudinal plasmon resonance agreed well with the width calculated using the Gans expression (quasi-static approximation).[25,26] No evidence for surface scattering was found,[15,16] which is not too surprising given the relatively large size of the particles. On the other hand, Guyot-Sionnest and co-workers studied the scattering spectra of nanorods with a gold core and a silver shell.[19] They found that adding a silver shell produces a significant increase in the width of the longitudinal plasmon band of the rods (30−40% increase at 1.8 eV resonance energy), which they attributed to scattering at the interface between the silver and gold.[19]

In this paper, we present the results and a simple analysis of the scattering spectra from bimetallic gold−silver particles with an approximately spherical shape. Both core−shell and alloyed particles have been examined. The average diameters of the particles in these experiments were between 40 and 60 nm. These sizes are large enough that scattering at the particle solution interface should not be important but not too large that retardation effects make a significant contribution to the width of the plasmon resonance. (This issue will be examined below through Mie theory calculations.) The plasmon resonances of these particles are much broader than those observed by Guyot-Sionnest and co-workers.[19] However, we believe that this broadening mainly arises from the frequency dependence of the dielectric constants of the particles[1] and not (in the case of the core−shell particles) from scattering at the interface between the two metals. In addition to fundamental issues about electron scattering, there is considerable interest in using Au−Ag core−shell particles as substrates for surface-enhanced Raman scattering (SERS).[27] The scattering spectra recorded here show how the position and width of the plasmon resonance depend on the ratio of Au to Ag and the particle geometry. This in turn provides information about the electric field enhancements at the particle surface, which are relevant to SERS.

2. Experimental Section

(a) Particle Synthesis. Core−shell particles were synthesized in two steps. First, 40 nm diameter (16% polydispersity) Au core particles were synthesized and then a Ag shell was deposited on the preformed Au seeds. The Au particles were made using a modified Turkevich recipe (lower [citrate]/[Au] ratio than that usually used in the Turkevich method).[28,29] Briefly, 450 mL of water containing about 0.05 g of $HAuCl_4 \cdot 3H_2O$ (Aldrich) was heated to boiling, and 10 mL of 0.01 M sodium citrate was added to the boiling solution under vigorous stirring. The solution was boiled for an additional 30 min, and the volume was adjusted to 500 mL after cooling. The Au sol obtained had a plasmon band at 531 nm and a gold concentration of $\sim 2.5 \times 10^{-4}$ M.

The Ag shell was deposited onto the Au seed particles using the radiolytic method developed by Henglein and co-workers.[30] The 40 nm Au seed and a $KAg(CN)_2$ solution were deaerated with Ar for 20 min and then mixed in a glovebox under Ar. The mixture was placed in a 100 mL glass vessel which had two septa and carried a sidearm with an optical cuvette. This mixture contained 1×10^{-4} M Au, 0.5 M methanol, 0.01 M PVP (Calbiochem, MW = 40 000 g mol^{-1}), and different amounts of $KAg(CN)_2$ (depending on the final desired ratio of Au/Ag). The solution was then flushed with ultrapure N_2O gas for 5 min to eliminate aqueous electrons formed during irradiation (which can create new Ag particles). Next, the solution was irradiated by a ^{60}Co-γ source at a dose rate of either 39 krad/h or 1.3×10^2 krad/h. The irradiation time varied from 50 to 200 min depending on the thickness of the Ag shell and the dose rate used. UV−vis absorption spectra were taken during the irradiation, and the complete reduction was confirmed when no further change in the UV−vis spectra could be noticed. Following the irradiation, a small amount of Amberlite MB-150 ion-exchange resin (Aldrich) was used to remove excess cyanide ion and the mixture was gently shaken overnight.

The particles were analyzed by TEM (using a JEOL JEM-100SX electron microscope at 100 kV accelerating voltage) and UV−vis absorption spectroscopy (Cary 50 Bio UV−vis spectrophotometer). Representative TEM images of particles used in these experiments are presented in the Supporting Information for this paper. Analysis of the TEM images showed that the gold core particles were slightly elliptical, with an average aspect ratio of 1.3. The particles increased in size, and the aspect ratio decreased slightly upon the addition of silver. The ratios of Au to Ag used to make the Au(core)−Ag(shell) particles were 1:0.05, 1:0.2, 1:0.5, 1:1, and 1:2. These ratios gave average shell thicknesses of 1, 2, 3, 6, and 8 nm (all ±20% errors), respectively, as determined by the increase in size observed by TEM. The measured shell thicknesses are in excellent agreement with the expected increase in size based on the mole ratios of Au to Ag, implying that most of the Ag is deposited onto the Au core particles.

Ag particles with a 26 nm diameter (12% polydispersity) were synthesized radiolytically by enlargement of Ag seeds. To synthesize the Ag seed particles, a 50 mL solution containing 1×10^{-4} M $AgClO_4$, 1.5×10^{-3} M potassium polyvinyl sulfate (Serva, MW = 245 000 g mol^{-1}), and 0.5 M methanol was irradiated for 60 min at a dose rate of 1.3×10^2 krad/h. The Ag seeds were then mixed with $KAg(CN)_2$ solution under Ar to form a mixture which contained 1×10^{-5} M Ag seed, 4×10^{-3} M $KAg(CN)_2$, 2×10^{-4} M sodium citrate, 2×10^{-2} M poly(vinyl alcohol) (PVA, Aldrich, MW = 50 000−85 000 g mol^{-1}), and 0.5 M methanol. Similar with the above Au(core)−Ag(shell) particle synthesis, after saturation with N_2O and γ-irradiation of the mixture, ion-exchange resin was added in the solution and the mixture was shaken overnight to remove the cyanide ions. The enlarged Ag sol had a diameter of about 26 nm with a narrow size distribution and spherical shape as determined by TEM analysis. The 26 nm Ag particles were coated with Au shells with different thicknesses. The strategy to synthesize the Ag(core)−Au(shell) particles is similar to that of the Au(core)−Ag(shell) particles. The difference is that, for the Ag(core)−Au(shell) particles, no PVP stabilizer was added and the Ag seeds were mixed with $KAu(CN)_2$ instead of $KAg(CN)_2$. The ratios of Ag to Au used to make the Ag(core)−Au(shell) particles were 1:0.05 and 1:0.2. UV−vis absorption spectra for the seed particles and several core−shell particles are presented in Figure 1. The spectra of the core−shell particle agree well with previous results.[30−32] Note especially the double peak structure for the Au(core)−Ag(shell) particles.

Alloyed nanoparticles were produced by laser-induced heating of the core−shell particles,[33] using the 532 nm output of a Continuum Surelite I, Q-Switched Nd:YAG laser. The repetition rate was 10 Hz with pulse energies of <5 mJ/pulse. The samples were irradiated for several hours, until the spectra did not show any further changes. These fairly gentle excitation conditions ensure that the particles are not fragmented during irradiation.[33] The spectra of the alloyed particles (which are are given in the Supporting Information) show a single plasmon resonance between the plasmon bands of pure gold and pure silver, consistent with previous results.[33,34]

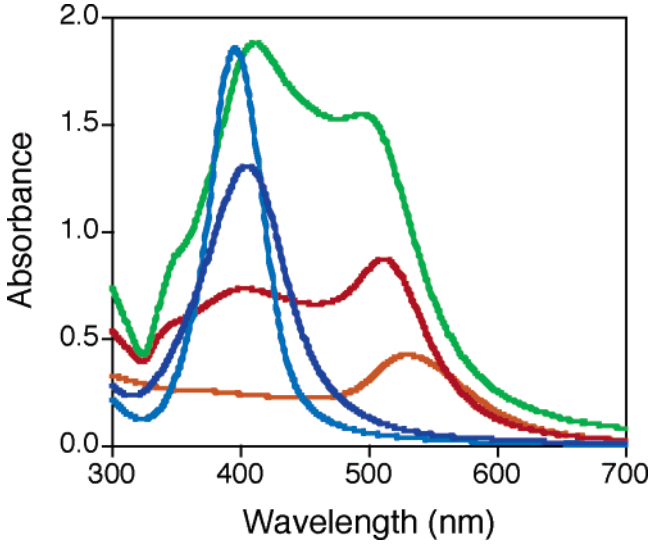

Figure 1. Extinction spectra of 40 nm gold seed particles (orange), 26 nm Ag seed particles (blue), 1:0.5 Au(core)−Ag(shell) particles (red), 1:2 Au(core)−Ag(shell) particles (green), and 1:0.2 Ag(core)−Au(shell) particles (purple).

(b) Single Particle Spectroscopy. Spectra of single particles were recorded using an Olympus IX-71 inverted optical microscope set up for dark-field microscopy. Specifically, the samples were dispersed at low concentration on a glass microscope slide and illuminated by the unpolarized output of a 100 W halogen lamp, with a dark-field oil-immersion condenser (Olympus U-DCW). The scattered light was collected with a 60x objective and directed to an imaging monochromator (Acton Research MicroSpec 2150i). The light transmitted by the microscope was dispersed by the monochromator and imaged onto a Roper Scientific 100 × 1340 B liquid N_2 cooled CCD camera. Normalized Rayleigh scattering spectra from individual particles were obtained by subtracting and dividing by a background, which was taken from a nearby region of the CCD camera. Typical acquisition times for the spectra were 10 s to 1 min, depending on the sample (particles with a large amount of Ag are much brighter the Au particles).

The width and resonance frequency of the plasmon band was obtained by fitting the scattering spectra to a Lorentzian function, using the Solver Routine in Microsoft Excel. Only particles with a smooth and relatively symmetrical resonance were included in our analysis. In many cases (especially for the bimetallic particles), a linearly increasing baseline (in energy) was added to fit the data. As will be shown below by comparison to calculated spectra, this is a property of the particles and not an instrumental artifact. Scattering spectra were calculated using Mathematica (version 5.1).

3. Results and Discussion

(a) Calculated Scattering Spectra for Core−Shell Particles. Before presenting the experimental results, it is important to understand what to expect from the Rayleigh scattering measurements. Figure 2a shows calculated spectra for Au(core)−Ag(shell) particles with a 20 nm radius Au core and Ag shells of different thicknesses. Figure 2b shows analogous calculations for Ag(core)−Au(shell) particles. These spectra were calculated using the theory developed by Kerker,[35,36] which takes into account retardation effects. This is an important issue in these experiments: adding a shell increases the size of the particles and may lead to broadening simply from electromagnetic retardation. Such broadening, which has nothing to do with

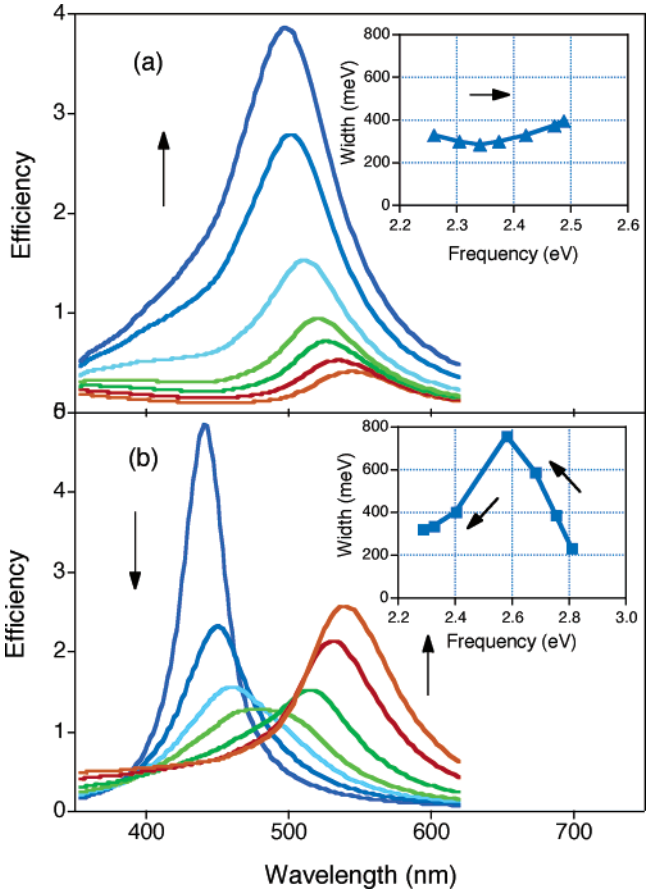

Figure 2. (a) Calculated scattering spectra for Au(core)−Ag(shell) particles, with a 40 nm diameter gold core and Ag shells with 1, 2, 3, 5, 8, and 10 nm thicknesses. The insert shows the line width plotted against the resonance frequency. The arrows indicate increasing shell thickness. (b) Calculated scattering spectra for Ag(core)−Au(shell) particles, with a 40 nm diameter Ag core and Au shells with 1, 2, 3, 5, 8, and 10 nm thicknesses.

scattering at the metal interface, can potentially be misleading in interpreting the experimental results. Specifically, the scattering efficiency Q_{sca} is obtained from[1,24,35,36]

$$Q_{sca} = \frac{2}{y^2}\sum_{n=1}^{\infty}(2n+1)\{|a_n|^2 + |b_n|^2\} \tag{2}$$

where the a_n and b_n coefficients are given by

$$a_n = \frac{\psi_n(y)[\psi'_n(m_2y) - A_n\chi'_n(m_2y)] - m_2\psi'_n(y)[\psi_n(m_2y) - A_n\chi_n(m_2y)]}{\xi_n(y)[\psi'_n(m_2y) - A_n\chi'_n(m_2y)] - m_2\xi'_n(y)[\psi_n(m_2y) - A_n\chi_n(m_2y)]} \tag{3a}$$

$$b_n = \frac{m_2\psi_n(y)[\psi'_n(m_2y) - B_n\chi'_n(m_2y)] - \psi'_n(y)[\psi_n(m_2y) - B_n\chi_n(m_2y)]}{m_2\xi_n(y)[\psi'_n(m_2y) - B_n\chi'_n(m_2y)] - \xi'_n(y)[\psi_n(m_2y) - B_n\chi_n(m_2y)]} \tag{3b}$$

and

$$A_n = \frac{m_2\psi'_n(m_1x)\psi_n(m_2x) - m_1\psi_n(m_1x)\psi'_n(m_2x)}{m_2\psi'_n(m_1x)\chi_n(m_2x) - m_1\psi_n(m_1x)\chi'_n(m_2x)} \tag{3c}$$

$$B_n = \frac{m_2\psi_n(m_1x)\psi'_n(m_2x) - m_1\psi_n(m_2x)\psi'_n(m_1x)}{m_2\psi_n(m_1x)\chi'_n(m_2x) - m_1\psi'_n(m_1x)\chi_n(m_2x)} \tag{3d}$$

where $x = ka$, $y = kb$, a is the radius of the core, b is the total radius, $m_i = n_i/n_{med}$ ($i = 1$ for the core and 2 for the shell), and $\psi_n(z) = zj_n(z)$, $\xi_n(z) = zh_n^{(1)}(z)$ and $\chi_n(z) = -zy_n(z)$ are the Riccati−Bessel functions. The refractive index of the medium was set to 1.5 for the calculations presented in Figure 2. The refractive indexes of Ag and Au were calculated from the dielectric constant data given by Quinten.[37] No correction has been made for surface (or interface) scattering in these calculations.

For the gold core particles, the calculated scattering spectra show a single peak that shifts to the blue as the amount of Ag increases. The inset of Figure 2a shows the width of the peak plotted against the resonance frequency. The width is on the order of 300 meV, which is consistent with the results from refs 15 and 16. The blue shift in the Au(core)−Ag(shell) spectra with increasing thickness of the silver shell is expected based on the experimental absorption spectra (see Figure 1) and previous studies of core−shell particles.[30−33] Interestingly, the width initially decreases slightly with increasing silver, up to a shell thickness of approximately 2 nm, and then increases. Note that the change in line width with added Ag is quite small (<50 meV), which means that broadening due to radiation damping should not be a major problem in our experiments.

The width of the plasmon resonance in the absence of surface scattering or radiation damping effects is primarily determined by the value of ϵ_2 for the particles. The decrease in the width in Figure 2a for small amounts of added silver arises because the value of ϵ_2 for silver is much less than that for gold, especially in the spectral region where the plasmon resonance occurs for these particles.[37] This decreases the effective value of ϵ_2 for the particles and reduces the damping of the plasmon resonance. The small increase in width at a shell thickness greater than 2 nm could arise either from radiation damping (i.e., it is due to retardation effects)[1] or because of the blue shift in the spectra: for Au and Ag, ϵ_2 increases with a frequency in the 2−3 eV range due to the interband transitions. This will be discussed in more detail below.

The Ag(core)−Au(shell) spectra (Figure 2b) show a red shift and strong damping of the plasmon resonance with added gold, up to a shell thickness of 3 nm. The damping arises from the much larger value of ϵ_2 for gold compared to silver in the 400 to 500 nm spectral region.[37] At shell thicknesses greater than 3 nm there is a decrease in the calculated line width. This is because the spectral red shift for these particles is so large that their plasmon resonances have moved into a region where the values of ϵ_2 for the metals are relatively small.[37] For gold, the interband contribution to the imaginary component of the dielectric constant decreases rapidly for wavelengths longer than 500 nm.

Surface scattering can be simply included in these calculations by modifying the intraband contribution to the dielectric constant, as discussed above. Specifically, subtracting the Drude model expressions for ϵ_1 and ϵ_2 with $\gamma = \gamma_b$ from the experimental dielectric constants and adding it back with surface scattering included yields

$$\epsilon_1(\omega) \approx \epsilon_1^{\text{bulk}}(\omega) \tag{4a}$$

$$\epsilon_2(\omega) \approx \epsilon_2^{\text{bulk}}(\omega) + \frac{\omega_p^2}{\omega^3} \times \frac{Av_F}{L_{\text{eff}}} \tag{4b}$$

where we have made the approximation that $\omega \gg \gamma$.[37] For the core, $L_{\text{eff}} = 1.333R$, and for the shell, $L_{\text{eff}} \approx 2d$, where d is the shell thickness.[13] Calculations were performed using a value of

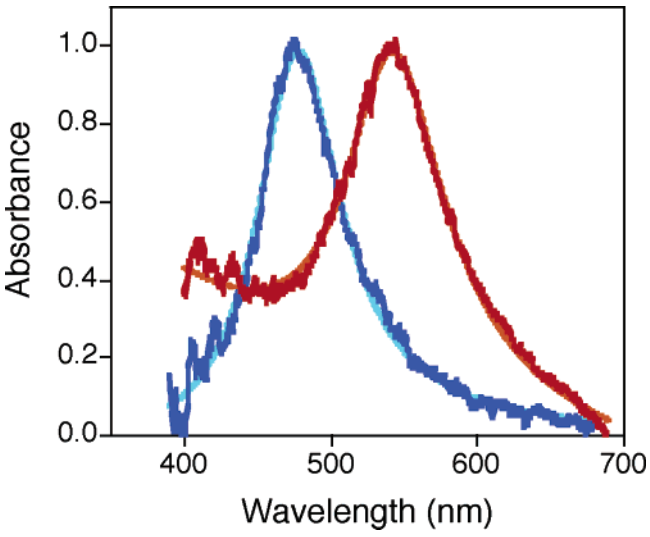

Figure 3. Rayleigh scattering spectra for bimetallic gold−silver particles formed from 40 nm diameter Au particles with (nominally) equal amounts of gold and silver. The red spectrum corresponds to a core−shell particle, and the blue spectrum corresponds to an alloyed particle. Fits to the spectra using a Lorentzian function are also presented.

$A = 1$ for both interfaces (metal−metal and metal−solution). This is somewhat larger than the values inferred by Guyot-Sionnest and co-workers and, therefore, should overestimate the effect of interface damping.[19] The calculated spectra are very similar to those presented in Figure 2. The spectral widths obtained including the size correction term (i.e., the $\omega_p^2 Av_F/\omega^3 L_{\text{eff}}$ term in eq 4b) are approximately 15% larger than those calculated without interface damping for a shell thickness of 1 nm (this is the thinnest shell examined in this work and, therefore, will give the largest effect).

The relative effect of the interface calculated using eqs 2−4 is much smaller than that observed in ref 19 for two reasons—both of which are due to the fact that the plasmon resonances for spherical particles are at higher frequencies than those for rods. First, the values of ϵ_2 for the bulk metals are much larger in the frequency range where the plasmon resonance occurs for spherical particles, due to the contribution from the interband transitions. This means that the spectra are broader and, therefore, the relative change from surface scattering is less. Second, the $1/\omega^3$ factor that appears in the size correction term attenuates the contribution from interface damping to ϵ_2 at higher frequencies.

(b) Experimental Scattering Spectra. Examples of Rayleigh scattering spectra from single particles are presented in Figure 3 for particles with (nominally) equal amounts of gold and silver. The spectrum with a resonance at 485 nm corresponds to a particle with an alloyed geometry, and the spectrum with the resonance at 550 nm is a Au(core)−Ag(shell) particle. The shape of the core−shell spectra (i.e., a resonance on a sloping baseline) is in reasonable agreement with the calculated spectra in Figure 2a. Figure 4 shows a plot of the width of the resonances vs the resonance frequency for particles formed from a gold core. The top panel shows the results for the core−shell geometry particles, and the bottom panel shows the data for alloyed particles. Corresponding data for particles synthesized with a Ag core are presented in Figure 5 (top panel = core−shell and bottom panel = alloyed).

There are several features to note about the experimental data. First, there is a wide variation in both the resonance frequency and the measured widths for all the samples. The variations in

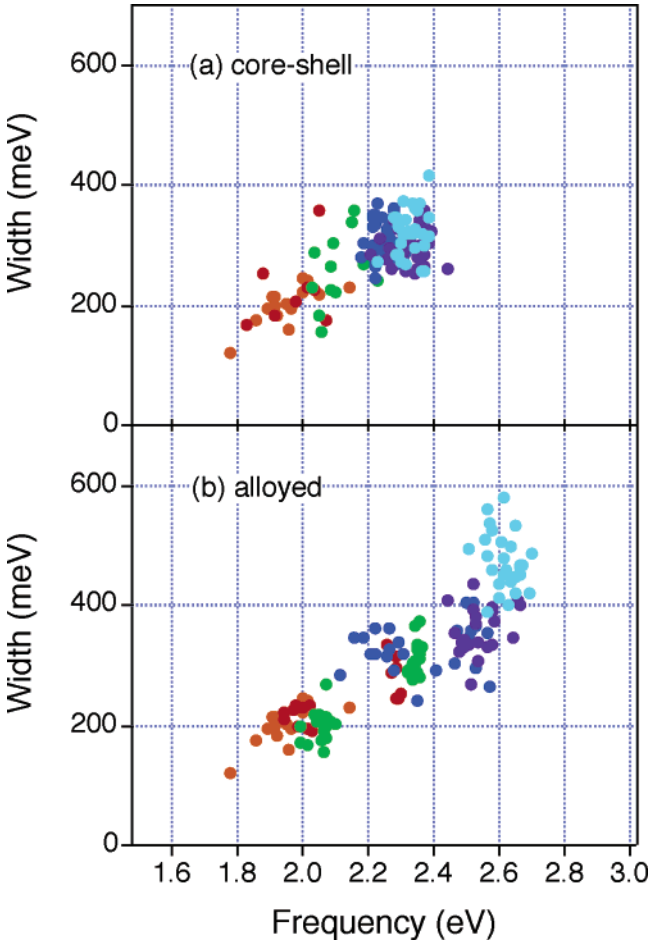

Figure 4. Line width vs resonance energy for (a) Au(core)−Ag(shell) particles and (b) alloyed particles formed from a 40 nm gold core: orange = pure gold, red = 1:0.05 Au/Ag, green = 1:0.2 Au/Ag, dark blue = 1:0.5 Au/Ag, purple = 1:1 Au/Ag, and light blue = 1:2 Au/Ag.

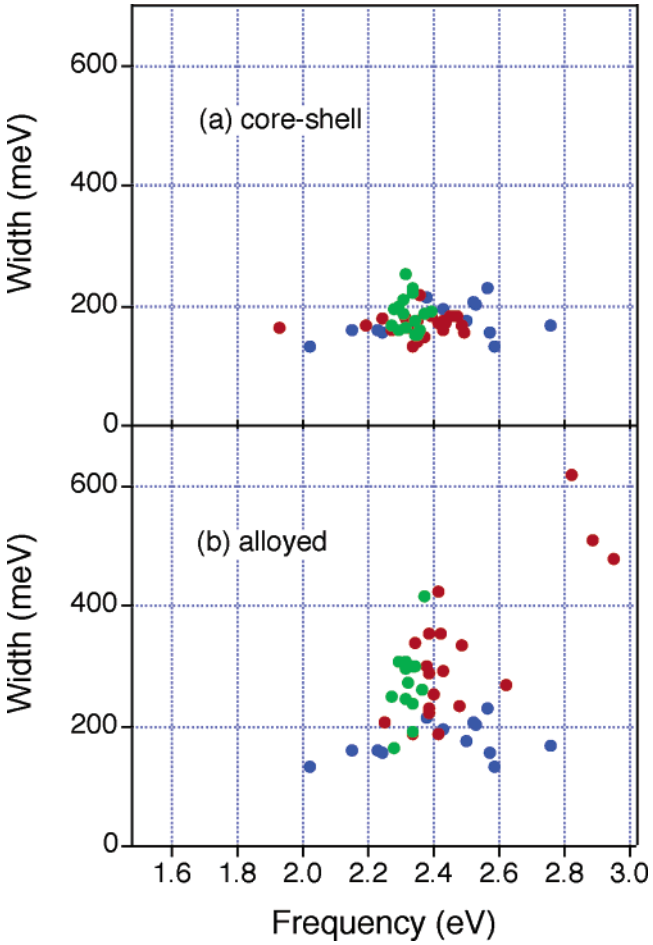

Figure 5. Line width vs resonance energy for (a) Ag(core)−Au(shell) particles and (b) alloyed particles formed from a 26 nm silver core: blue = pure silver, red = 1:0.05 Ag/Au, and green = 1:0.2 Ag/Au.

the resonance frequency arise from several factors. First, the particles in these experiments have a variety of shapes. It is well-known that ellipsoidal- and triangular-shaped particles have red-shifted plasmon resonances compared to spherical particles.[1,17,26,38] In addition, the particles also experience variations in the effective refractive index of their environment.[18] Finally, different particles in a given sample will have different proportions of silver and gold. This is particularly noticeable for the alloyed particles formed from a gold core. For example, the sample with a Au-to-Ag ratio of 1:0.2 shows two distinct data sets: one centered at a 2.05 eV resonance frequency and one at 2.34 eV. The alloyed particles formed by laser-induced heating should be spherical; thus, this implies that there are two subsets of particles in the sample with different amounts of Ag. Similarly, the sample with a Au-to-Ag ratio of 1:0.5 also shows two sets of resonance frequencies, one at 2.25 eV and one at 2.52 eV. Note that in both cases the majority of the particles observed under the microscope correspond to the higher energy resonance (the number of points in Figure 4b does not represent the percentage of particles of a given type).

In general, the data shows that the width of the resonance in the scattering spectra increases with resonance frequency. The exception is the Ag(core)−Au(shell) particles in Figure 5a, where the width is constant over a wide frequency range. The calculations presented in Figure 2b show that adding a small amount of gold to a silver core strongly decreases the amplitude of the plasmon resonance and increases the width. The decrease in intensity creates a bias in the optical experiments toward particles with little or no gold (it is natural to select the brightest particles for analysis). Thus, we do not believe that the Ag(core)−Au(shell) data in Figure 5a truly represent core−shell particles, and these data will not be analyzed further.

To try and understand the trends in the data, the average width determined from the single particle experiments is plotted against the average resonance frequency in Figure 6. The errors bars in the figure represent the standard deviation of the data. Note that two points are given for the 1:0.2 and 1:0.5 Au(core)−Ag(shell) particles, which show a bimodal distribution of resonance frequencies. Figure 6 clearly shows that for a given resonance frequency the width of the plasmon band for the core−shell particles is essentially identical to that of the alloyed particles. Thus, the interface between the two metals does not cause any measurable increase in the damping of the plasmon oscillation in this system. On the other hand, for a given Au-to-Ag ratio, the alloyed particles give broader resonances than the core−shell particles. This is because the plasmon bands for the alloyed particles are shifted to higher frequencies and the contribution from interband damping increases with frequency.

The way the width changes with resonance frequency can be calculated using the expression derived by Kreibig[1,37,39]

$$\Gamma = \frac{2\epsilon_2}{|(d\epsilon_1/d\omega)|} \tag{5}$$

where we have used the approximation that $|(d\epsilon_1/d\omega)| \gg$

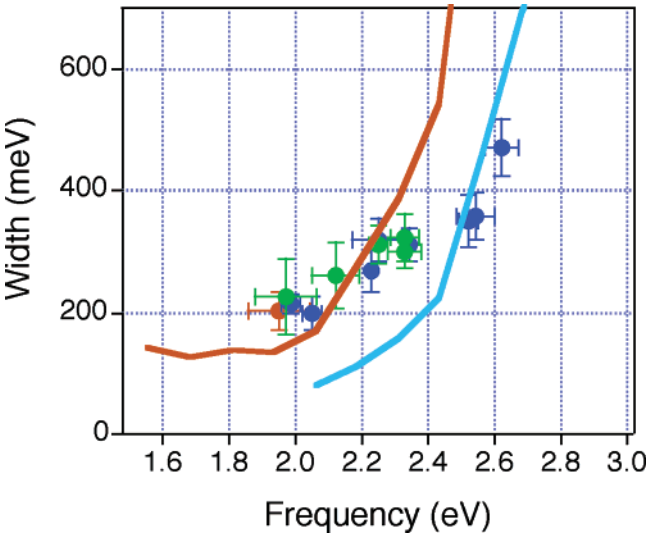

Figure 6. Average line width vs average resonance energy for the data presented in Figures 4 and 5: dark blue = alloyed, green = core−shell, and orange = pure gold. The lines indicate the line widths calculated using eq 5: orange = 40 nm diameter gold particles and light blue = 56 nm diameter particles with a 1:2 ratio of Au/Ag. See text for details.

$|(d\epsilon_2/d\omega)|$.[37] This expression does not take into account broadening from retardation effects. Calculated values of Γ for pure gold and 1:2 Au/Ag particles are presented in Figure 6. In these calculations, the surface damping parameter A was set to $A = 1$ and L_{eff} was taken to be $^4/_3$ times the total radius of the particle (i.e., we simply treat the particle as a homogeneous sphere). For Au, this value of A is slightly larger than the value determined in our previous work[40] but within the range of values given by Quinten.[37] The dielectric constants of the composite particles were calculated by simply averaging the dielectric constants of Au and Ag. The calculations do a reasonable job of matching the experimental data at high energy (particles with a large percentage of silver). This shows that the increases in line width with resonance frequency are simply due to the frequency dependence of the dielectric constants; specifically, the onset of the interband transitions in Au in the 2 eV region causes an increase in ϵ_2 and, therefore, an increase in the damping constant.

At lower energies, the agreement between the calculated and experimental data is not as good. The experimental data is consistently higher than the calculated line widths. This was also observed in the work of Sonnichsen et al.[16] This could indicate that it is not appropriate to neglect retardation effects/radiation damping, even though the calculations in Figure 2 show that this should be a negligible effect. It could also be an artifact from the fact that our particles are not perfectly spherical. However, because our data is consistent with that of ref 16, where only optically spherical particles were included in the analysis, we do not believe that the nonspherical shape of the particles is a major problem. (Experiments with polarized light are currently underway to examine this issue.) It is also possible that the dielectric constants used in the calculations are not quite right. For example, the dielectric constants determined by Quinten (ref 37) are very different to those of Johnson and Christy,[41] especially in the interband region. The reason the dielectric constant data of Quinten was used in the present study, rather than the Johnson and Christy values, is that Sonnichsen et al. showed that the Quinten data gives a much better agreement with the measured line widths for silver particles.[16] Note that good agreement between the experimental and calculated line widths in our measurements can be obtained by setting the surface scattering parameter to $A = 3$, which seems to be too large from previous studies.[1,37]

4. Summary and Conclusions

The optical scattering spectra for single particles of pure Au and Ag, core−shell Au−Ag particles, and alloyed particles have been examined by dark-field microscopy. The results show that, starting with a gold core, the width of the plasmon resonance increases as the amount of silver increases. For a given resonance frequency, the line widths for the alloyed particles are very similar to those of the core−shell particles. This indicates that scattering at the interface between the two metals does not significantly affect the damping of the plasmon resonance for this system (gold and silver particles with an approximately spherical geometry). Calculations of the line width vs resonance frequency using the dielectric constants for silver and gold determined by Quinten (ref 37) are in reasonable agreement with the experimental data. This demonstrates that the increase in line width with increasing resonance frequency is simply due to the way the dielectric constants change with frequency. Specifically, the onset of the interband transitions in Au at 2 eV causes an increase in the imaginary component of the dielectric constant and, therefore, an increase in the damping of the collective electron oscillation in bimetallic Au−Ag particles.

The conclusion that electron scattering at the interface between the two metals does not significantly affect the line width of the plasmon resonance is opposite to the results of Guyot-Sionnest and co-workers.[19] However, these workers examined rod-shaped particles (gold core−silver shell), which had plasmon resonances <2.1 eV. This has two important consequences. First, the interband transitions in gold make a much smaller contribution to the dielectric constant,[37] which means smaller line widths and makes it easier to see changes induced by surface scattering. Second, the surface scattering term scales as $1/\omega^3$, see eq 4, which means that interface damping effects are more pronounced at lower resonance frequencies. Thus, our results do not necessarily contradict those of Guyot-Sionnest and co-workers.[19]

Acknowledgment. This work is supported by the United States National Science Foundation (Grant No. CHE02-36279) and the Petroleum Research Fund (Grant No. PRF-39761AC) administered by the American Chemical Society.

Supporting Information Available: TEM images and UV−vis absorption spectra of Au(core)−Ag(shell) particles and UV−vis absorption spectra of Au and Ag seed particles and alloyed particles. This material is available free of charge via the Internet at http://pubs.acs.org.

References and Notes

(1) Kreibig, U.; Vollmer, M. *Optical Properties of Metal Clusters*; Springer: Berlin, 1995.
(2) Fragstein, C. v.; Römer, H. *Z. Phys.* **1958**, *151*, 54.
(3) Hampe, W. *Z. Phys.* **1958**, *152*, 476.
(4) Doyle, W. T. *Phys. Rev.* **1958**, *111*, 1067.
(5) Doremus, R. H. *J. Chem. Phys.* **1964**, *40*, 2389.
(6) Doremus, R. H. *J. Chem. Phys.* **1965**, *42*, 414.
(7) Euler, J. *Z. Phys.* **1954**, *137*, 318.
(8) Kreibig, U.; Fragstein, C. v. *Z. Phys.* **1969**, *224*, 307.
(9) Krauss, W. A.; Schatz, G. C. *Chem. Phys. Lett.* **1983**, *99*, 353.
(10) Krauss, W. A.; Schatz, G. C. *J. Chem. Phys.* **1983**, *79*, 6130.
(11) See refs 18 and 19 of Quinten, M. *Z. Phys. B: Condens. Matter* **1996**, *101*, 211.

(12) Ashcroft. N. W.; Mermin, N. D. *Solid State Physics*; Holt, Rinehart and Winston: New York, 1976.
(13) Coronado, E. A.; Schatz, G. C. *J. Chem. Phys.* **2003**, *119*, 3926.
(14) Sonnichsen, C.; Geier, S.; Hecker, N. E.; von Plessen, G.; Feldmann, J.; Ditlbacher, H.; Lamprecht, B.; Krenn, J. R.; Aussenegg, F. R.; Chan, V. Z. H.; Spatz, J. P.; Moller, M. *Appl. Phys. Lett.* **2000**, *77*, 2949.
(15) Sonnichsen, C.; Franzl, T.; Wilk, T.; von Plessen, G.; Feldmann, J.; Wilson, O.; Mulvaney, P. *Phys. Rev. Lett.* **2002**, *88*, 077402.
(16) Sonnichsen, C.; Franzl, T.; Wilk, T.; von Plessen, G.; Feldmann, J. *New J. Phys.* **2002**, *4*, 93.
(17) Mock, J. J.; Barbic, M.; Smith, D. R.; Schultz, D. A.; Schultz, S. *J. Chem. Phys.* **2002**, *116*, 6755.
(18) Mock, J. J.; Smith, D. R.; Schultz, S. *Nano Lett.* **2003**, *3*, 485
(19) Liu, M. Z.; Guyot-Sionnest, P. *J. Phys. Chem. B* **2004**, *108*, 5882.
(20) Boyer, D.; Tamarat, P.; Maali. A.; Lounis, B.; Orrit, M. *Science* **2002**, *297*, 1160.
(21) Lindfors, K.; Kalkbrenner, T.; Stoller, P.; Sandoghdar, V. *Phys. Rev. Lett.* **2004**, *93*, 037401.
(22) Arbouet, A.; Christofilos, D.; Del Fatti, N.; Vallee, F.; Huntzinger, J. R.; Arnaud, L.; Billaud, P.; Broyer, M. *Phys. Rev. Lett.* **2004**, *93*, 127401.
(23) Berciaud, S.; Cognet, L.; Tamarat, P.; Lounis, B. *Nano Lett.* **2005**, *5*, 515.
(24) van de Hulst, H. C. *Light Scattering by Small Particles*; Dover Publications: New York, 1981.
(25) Gans, R. *Ann. Phys.* **1915**, *47*, 270.
(26) (a) Link, S.; Mohamed, M. B.; El-Sayed, M. A. *J. Phys. Chem. B* **1999**, *103*, 3073. (b) Link, S.; El-Sayed, M. A.; Mohamed, M. B. *J. Phys. Chem. B* **2005**, *109*. 10531.
(27) Freeman, R. G.; Grabar, K. C.; Allison, K. J.; Bright, R. M.; Davis, J. A.; Guthrie, A. P.; Hommer, M. B.; Jackson, M. A.; Smith, P. C.; Walter, D. G.; Natan, M. J. *Science* **1995**, *267*, 1629.
(28) Turkevich, J.; Stevenson, P. C.; Hillier, J. *Discuss. Faraday Soc.* **1951**, *11*, 55.
(29) Frens, G. *Nat. Phys. Sci.* **1973**, *241*, 20.
(30) (a) Mulvaney, P.; Giersig, M.; Henglein, A. *J. Phys. Chem.* **1993**, *97*, 7061. (b) Henglein, A.; Meisel, D. *Langmuir* **1998**, *14*, 7392.
(31) Kim, Y.; Johnson, R. C.; Li, J.; Hupp, J. T.; Schatz, G. C. *Chem. Phys. Lett.* **2002**, *352*, 421.
(32) Moskovits, M.; Srnova-Sloufova, I.; Vlckova, B. *J. Chem. Phys.* **2002**, *116*, 10435.
(33) Hodak, J. H.; Henglein, A.; Giersig, M.; Hartland, G. V. *J. Phys. Chem. B* **2000**, *104*, 11708.
(34) Link, S.; Wang, Z. L.; El-Sayed, M. A. *J. Phys. Chem.* **1999**, *103*, 3529.
(35) Kerker, M. *The Scattering of Light and Other Electromagnetic Radiation*; Academic Press: New York, 1969.
(36) Bohren, C. F.; Huffman, D. R. *Absorption and Scattering of Light by Small Particles*; Wiley-Interscience: New York, 1983.
(37) Quinten, M. *Z. Phys. B: Condens. Matter* **1996**, *101*, 211.
(38) Jin, R. C.; Cao, Y. C.; Hao, E. C.; Metraux, G. S.; Schatz, G. C.; Mirkin, C. A. *Nature* **2003**, *425*, 487.
(39) Kreibig, U. *Appl. Phys.* **1976**, *10*, 255.
(40) Hodak, J. H.; Henglein, A.; Hartland, G. V. *J. Phys. Chem. B* **2000**, *104*, 9954.
(41) Johnson, P. B.; Christy, R. W. *Phys. Rev. B* **1972**, *6*, 4370.